PDE-Based Feedback Control of Freeway Traffic Flow via Time-Gap Manipulation of ACC-Equipped Vehicles

Nikolaos Bekiaris-Liberis and Argiris I. Delis

***Abstract*— We develop a control design for stabilization of traffic flow in the congested regime, based on an Aw-Rascle-Zhang-type (ARZ-type) partial differential equation (PDE) model, for traffic consisting of both adaptive cruise control-equipped (ACC-equipped) and manual vehicles. The control input is the value of the time-gap setting of ACC-equipped and connected vehicles, which gives rise to a problem of control of a 2 × 2 nonlinear system of the first-order hyperbolic PDEs with in-domain actuation. The feedback law is designed in order to stabilize the linearized system, around a uniform, congested equilibrium profile. The stability of the closed-loop system under the developed control law is shown in constructing a Lyapunov functional. Convective stability is also proved to adopt an input-output approach. The performance improvement of the closed-loop system under the proposed strategy is illustrated in simulation, also employing three different metrics, which quantifies the performance in terms of fuel consumption, total travel time, and comfort.**

***Index Terms*— Adaptive cruise control (ACC), Aw-Rascle-Zhang (ARZ) model, connected and automated vehicles, hyperbolic systems, partial differential equation (PDE) control, traffic flow control.**

I. Introduction

ALTHOUGH traffic congestion may be unavoidable nowadays, due to the continuous increase in the number of vehicles and in the traffic demand, some of its ramifications may be alleviated employing real-time traffic control strategies [9]. Among other reasons, certain traffic flow instability phenomena, such as, for example, stop-and-go waves, are some of the causes of traffic congestion's negative consequences on fuel consumption, total travel time (TTT), drivers' comfort, and safety [44]. One promising avenue to traffic flow stabilization is the development of control design tools that exploit the capabilities of automated and connected vehicles [17] while retaining the distributed nature of traffic flow dynamics. It is the aim of this brief to develop a feedback law for traffic flow stabilization utilizing a partial differential equation (PDE) traffic flow model and exploiting the capabilities of adaptive cruise control-equipped (ACC-equipped) and connected vehicles.

Since the second-order, PDE traffic flow models (i.e., systems that incorporate two PDE states, one for traffic density and one for traffic speed) constitute realistic descriptions of the traffic dynamics, capturing important phenomena, such as, for example, stop-and-go traffic, capacity drop, etc., [15], [28], [33], boundary control designs are recently developed for such systems [6], [26], [28], [49], [50], [52], [53] and some of which are based on techniques originally developed for control of systems of hyperbolic PDEs, such as, for example, [12], [18], [25], [29], [31], [36], [46]. Even though simpler, first-order traffic flow models, in conservation law or Hamilton–Jacobi PDE formulation, are also important for modeling purposes. For this reason, PDE-based control design techniques exist for this class of systems as well [4], [7], [10], [16], [24], [30].

While most of the above PDE-based traffic control techniques rely on traditional implementation means such as ramp metering and variable speed limits, more rare are PDE-based, traffic flow control methodologies that exploit connected and automated vehicles capabilities. In particular, the work in [43], [45] develops control designs via in-domain manipulation of acceleration of ACC-equipped vehicles, considering traffic with only automated vehicles, and the work in [35], [48] develops control designs via speed manipulation of an autonomous vehicle. Furthermore, although in microscopic simulation it is reported that it may be beneficial for traffic flow to appropriately manipulate the ACC settings of vehicles already equipped with an ACC feature in real time [27], [39], [40], the problem of systematic feedback control design via time-gap manipulation has not, heretofore, been tackled from a PDE viewpoint.

In this brief, we design a feedback control strategy for stabilization of traffic flow in the congested regime, manipulating the time-gap setting of vehicles equipped with ACC and utilizing a control-oriented, Aw-Rascle-Zhang-type (ARZ-type) model with ACC (which is shown to possess certain important traffic flow-theoretic properties). The control strategy is developed for the linearized system around a uniform, congested equilibrium profile, which is proven to be open-loop unstable. Due to the presence (on average) of a certain penetration rate of ACC-equipped vehicles in a given freeway stretch, the traffic flow control problem is recast to the problem of stabilization of a 2×2 linear system of the first-order, heterodirectional hyperbolic PDEs with in-domain actuation. The closed-loop system under the proposed controller is shown to be exponentially stable (in C^1 norm), constructing a Lyapunov functional. We further

Manuscript received November 20, 2018; revised June 20, 2019; accepted January 15, 2020. Manuscript received in final form February 11, 2020. The work of Nikolaos Bekiaris-Liberis was supported by the European Commission's Horizon 2020 Research and Innovation Programme through the project PADECOT, Marie Sklodowska-Curie under Grant 747898. Recommended by Associate Editor C. Prieur. *(Corresponding author: Nikolaos Bekiaris-Liberis.)*

Nikolaos Bekiaris-Liberis is with the Department of Electrical and Computer Engineering, Technical University of Crete, 73100 Chania, Greece (e-mail: bekiaris-liberis@ece.tuc.gr).

Argiris I. Delis is with the Department of Production Engineering and Management, Technical University of Crete, 73100 Chania, Greece (e-mail: adelis@science.tuc.gr).

Color versions of one or more of the figures in this article are available online at http://ieeexplore.ieee.org.

Digital Object Identifier 10.1109/TCST.2020.2974148

study, employing an input-output approach, an additional stability property of the closed-loop system, namely convective stability, which is important from a traffic control point of view as it guarantees the nonamplification of speed perturbations, as these propagate upstream. The benefits in the traffic flow of employing the proposed strategy are illustrated in simulation, also including the quantification of the performance improvement in terms of various indices, measuring TTT, fuel consumption, and comfort level.

In Section II, we present a control-oriented traffic flow model for congested and mixed (i.e., consisting of both manual and ACC-equipped vehicles) traffic. In Section III, we introduce our feedback design, and in Section IV, we prove the stability and convective stability of the closed-loop system. The effectiveness of the proposed strategy is validated in the simulation in Section V. Concluding remarks and future research directions are provided in Section VI.

Notation: For scalar functions $u \in L^p(0, D)$, where p is a positive integer and $D > 0$, we define the norm $\|u\|_p = (\int_0^D |u(x)|^p dx)^{\frac{1}{p}}$ as well as the weighted norm $\|u\|_{\mu,p} = (\int_0^D e^{p\mu x}|u(x)|^p dx)^{\frac{1}{p}}$, for $\mu \neq 0$. For $u \in C[0, D]$, we denote $\|u\|_C = \max_{x\in[0,D]} |u(x)| = \lim_{p\to+\infty} \|u\|_p$ and $\|u\|_{\mu,C} = \max_{x\in[0,D]} |e^{\mu x}u(x)| = \lim_{p\to+\infty} \|u\|_{\mu,p}$. For $u \in C^1[0, D]$, we define $\|u\|_{C^1} = \|u\|_C + \|u'\|_C$ and, respectively, we define $\|u\|_{\mu,C^1} = \|u\|_{\mu,C} + \|u'\|_{\mu,C}$. For a signal $f \in \mathscr{L}_p$, we define its temporal norm $\|f\|_{\mathscr{L}_p} = (\int_0^{+\infty} |f(t)|^p dt)^{\frac{1}{p}}$, for $p < +\infty$, and $\|f\|_{\mathscr{L}_p} = \sup_{t\geq 0} |f(t)|$, for $p = +\infty$. The Laplace transform of a signal $f(t)$, $t \geq 0$, is denoted by $F(s)$.

II. ARZ-Type Model With ACC in Congested Regime

A. Description of the Model

We consider the following system:

$$\rho_t(x,t) = -\rho_x(x,t)v(x,t) - \rho(x,t)v_x(x,t) \tag{1}$$

$$v_t(x,t) = -\left(v(x,t) + \rho(x,t)\frac{\partial V_{\text{mix}}(\rho(x,t), h_{\text{acc}}(x,t))}{\partial\rho}\right) \times v_x(x,t) + \frac{V_{\text{mix}}(\rho(x,t), h_{\text{acc}}(x,t)) - v(x,t)}{\tau_{\text{mix}}} \tag{2}$$

$$q_{\text{in}} = \rho(0,t)v(0,t) \tag{3}$$

$$v_t(D,t) = \frac{V_{\text{mix}}(\rho(D,t), h_{\text{acc}}(D,t)) - v(D,t)}{\tau_{\text{mix}}} \tag{4}$$

where

$$V_{\text{mix}}(\rho, h_{\text{acc}}) = \tau_{\text{mix}}\left(\frac{\alpha}{\tau_{\text{acc}}}V_{\text{acc}}(\rho, h_{\text{acc}}) + \frac{1-\alpha}{\tau_m}V_m(\rho)\right) \tag{5}$$

$$V_{\text{acc}}(\rho, h_{\text{acc}}) = \frac{1}{h_{\text{acc}}}\left(\frac{1}{\rho} - L\right), \quad \rho_{\min} < \rho < \frac{1}{L} \tag{6}$$

$$V_m(\rho) = \frac{1}{h_m}\left(\frac{1}{\rho} - L\right), \quad \rho_{\min} < \rho < \frac{1}{L} \tag{7}$$

$$\tau_{\text{mix}} = \frac{1}{\frac{\alpha}{\tau_{\text{acc}}} + \frac{1-\alpha}{\tau_m}} \tag{8}$$

ρ is the traffic density, $v \in (0, v_{\text{f}}]$ is the traffic speed, with v_{f} being free-flow speed, $D > 0$ is the length of the freeway stretch, $L > 0$ is the average effective vehicle length, $\alpha \in [0, 1]$ is the percentage of ACC-equipped vehicles with respect to total vehicles, $\rho_{\min} > 0$ is the lowest density value for which the model is accurate,[1] $t \geq 0$ is time, $x \in [0, D]$ is the spatial variable, $q_{\text{in}} > 0$ is a constant external inflow, τ_{acc}, $\tau_m > 0$ are the time constants of ACC-equipped and manual vehicles, respectively, $h_m > 0$ is the time gap of manual vehicles, and $h_{\text{acc}} > 0$ is the time gap of ACC-equipped vehicles, which is the control input.[2]

B. Traffic Flow-Oriented Properties of the Model

Model (1)–(4) may be viewed as modification of the ARZ model such that traffic consisting of both manual and ACC-equipped vehicles can be handled, the time gap of ACC-equipped vehicles can be taken as manipulated variable, and a realistic downstream boundary condition is obtained.

1) Speed Dynamics: Equation (2) is inspired by the speed dynamics of ARZ model [51]. In fact, ARZ model may be viewed as both a model of traffic flow dynamics for traffic with only manual vehicles [51] as well as a model for traffic flow dynamics with only ACC-equipped vehicles [43]. For fixed time gaps of ACC-equipped vehicles, when $\alpha = 1$ (only ACC-equipped vehicles exist) or $\alpha = 0$ (only manual vehicles exist), the model reduces to the ARZ model with fundamental diagram given by (6) or (7), respectively, which correspond to the so-called constant time-gap policy (in analogy to the microscopic level), see, e.g., [8], [43], [45]. To account for the case of mixed traffic, i.e., when both manual and ACC-equipped vehicles are present, we define a new fundamental diagram relation as in (5), which is also written as

$$V_{\text{mix}}(\rho, h_{\text{acc}}) = \frac{1}{h_{\text{mix}}(h_{\text{acc}})}\left(\frac{1}{\rho} - L\right) \tag{9}$$

where the effective (or, mixed) time gap is defined as

$$h_{\text{mix}}(h_{\text{acc}}) = \frac{\alpha + (1-\alpha)\frac{\tau_{\text{acc}}}{\tau_m}}{\alpha + (1-\alpha)\frac{\tau_{\text{acc}}}{\tau_m}\frac{h_{\text{acc}}}{h_m}}h_{\text{acc}}. \tag{10}$$

2) Properties of the Mixed Fundamental Diagram: Fundamental diagram (9) retains the form (6), (7) while incorporating a different time gap. Therefore, in addition to inheriting the properties of the original fundamental diagrams, with respect to their dependence on density, the effect of the penetration rate of ACC-equipped vehicles is incorporated via the mixed time gap (10). This is illustrated in Fig. 1, showing the effect of the penetration rate to the actual (mixed) time gap. The mixed time gap may increase with respect to the penetration rate or decrease, depending on whether h_{acc} or h_m is larger. Furthermore, as long as $h_{\min} \leq \min\{h_{\text{acc}}, h_m\}$ and $\max\{h_{\text{acc}}, h_m\} \leq h_{\max}$, where $h_{\max}$ and $h_{\min}$ denote some maximum and minimum, respectively, possible time gaps,[3] it follows from (10) that h_{mix} satisfy $h_{\min} \leq \min\{h_{\text{acc}}, h_m\} \leq h_{\text{mix}} \leq \max\{h_{\text{acc}}, h_m\} \leq h_{\max}$, for all $\alpha \in [0, 1]$.

[1] One may view $\rho_{\min}$ as the critical density that corresponds to a minimum possible time-gap (see Section II-B).

[2] We consider continuously differentiable initial conditions satisfying the first-order compatibility with boundary conditions and, accordingly, employ in our analysis later on (see Section IV) the C^1 norm.

[3] For realistic values of $h_{\max}$ and $h_{\min}$ that may appear in practice see Section V as well as, e.g., [34], [40].

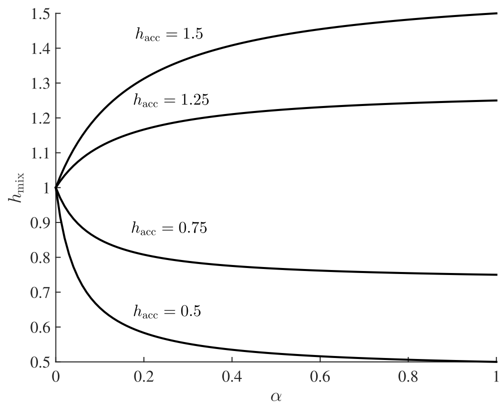

Fig. 1. Mixed time gap (10) for $h_m = 1$, $(\tau_{acc}/\tau_m) = 0.1$, and four different values of h_{acc}, as a function of the penetration rate α.

To better illustrate the form of the resulting mixed fundamental diagrams, for the various values of the mixed time gap, Fig. 2 shows an example of potentially meaningful fundamental diagrams (9)[4] for different (but fixed) values of h_{mix}. Specifically, $Q_{h_{min}}$ is fundamental diagram that corresponds to h_{min}, satisfying $h_{min} = (((1/\rho_{min}) - L)/v_f)$, defined as[5]

$$Q_{h_{min}}(\rho) = \begin{cases} v_f \rho, & 0 \le \rho \le \rho_{min} \\ \dfrac{1}{h_{min}}(1 - L\rho), & \rho_{min} < \rho \le \dfrac{1}{L}. \end{cases} \quad (11)$$

The fundamental diagram that corresponds to h_{max}, where h_{max} satisfies $h_{max} = (((1/\bar{\rho}_{min}) - L)/v_f)$, may be defined analogously. As it is evident in Fig. 2, all of the possible mixed fundamental diagrams that may appear, for any $\alpha \in [0, 1]$, lie between $Q_{h_{max}}$ and $Q_{h_{min}}$. This also implies that, as long as $\rho > \rho_{min} = (1/(L + v_f h_{min}))$, for every $h_{mix} \in [h_{min}, h_{max}]$ the resulting mixed fundamental diagram describes the congested traffic. Since for given values of v_f (dependent, for example, on the specific freeway stretch) and L, the requirements $\min\{h_{acc}, h_m\} \ge h_{min}$ and $\max\{h_{acc}, h_m\} \le h_{max}$ guarantee that $0 < V_{mix}(\rho, h_{acc}) < v_f$, for all $\alpha \in [0, 1]$ and $\rho_{min} < \rho < (1/L)$, relation (9) defines a reasonable fundamental diagram for mixed traffic in congested conditions.

3) Traffic Information Propagation: Since we are concerned with the case of congested traffic conditions we restrict our attention in a nonempty, connected open subset Ω of the set $\bar{\Omega} = \{(v, \rho, h_{acc}) \in \mathbb{R}^3 : 0 < v < v_f, (1/(L + v_f h_{min})) < \rho < (1/L), h_{min} \le h_{acc} \le h_{max}\}$, such that $v + \rho(\partial V_{mix}(\rho, h_{acc})/\partial\rho) < 0$, for all $\alpha \in [0, 1]$, whenever $(v, \rho, h_{acc}) \in \Omega$,[6] see, e.g., [6], [44]. Systems (1)–(4) are strictly hyperbolic with distinct, real nonzero eigenvalues $\lambda_1 = v$, $\lambda_2 = v + \rho(\partial V_{mix}(\rho, h_{acc})/\partial\rho) = v - (1/h_{mix}(h_{acc})\rho)$, as long as $(v, \rho, h_{acc}) \in \Omega$, which implies that information propagates forward with traffic flow at the traffic speed, whereas speed information travels backward. Thus, model (1)–(4) is anisotropic, see, e.g., [51].

[4]Although we restrict our attention to congested regime, and thus, it is sufficient to define only the right part (i.e., for $\frac{1}{L} > \rho > \rho_{min}$) of fundamental diagram (9), for completeness, we define a proper extension for the left part.

[5]Although $Q_{h_{min}}$ is not differentiable at ρ_{min}, one could obtain a differentiable approximation of the original fundamental diagram by adding an ϵ-layer around the critical density and defining $Q_{h_{min}}$ for $\rho \in [\rho_{min} - \epsilon, \rho_{min} + \epsilon]$ properly. Since we do not deal with free-flow conditions, in order to not distract the reader with additional technical details, we do not discuss this further.

[6]Provided that $\max\{h_{acc}, h_m\} \le h_{max}$, this holds true, for instance, for all $(v, \rho, h_{acc}) \in \bar{\Omega}$ in the special (but quite restrictive) case where $v_f \le (L/h_{max})$.

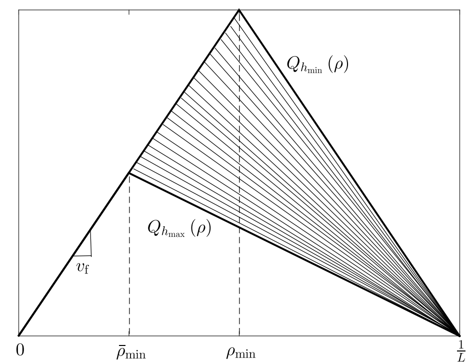

Fig. 2. Different fundamental diagrams (9) for $h_{mix} \in [h_{min}, h_{max}]$.

4) Boundary Condition at the Outlet: To obtain a realistic downstream boundary condition, in the sense that no additional control via ramp/mainline metering or variable speed limits is employed at the outlet of the controlled area of interest (which may be the end of a tunnel or the end of high-curvature or the end of an upgrade, etc.), as well as to obtain a well-posed system we impose the dynamic boundary condition (4), which implies free downstream traffic conditions, see also [26].

C. Equilibria of the System

The equilibria of system (1)–(4) dictated by a constant inflow q_{in} as well as a constant, steady-state time gap for ACC-equipped vehicles, say $\bar{h}_{acc}$, which results in a steady-state mixed time gap given by

$$\bar{h}_{mix} = \frac{\alpha + (1-\alpha)\frac{\tau_{acc}}{\tau_m}}{\alpha + (1-\alpha)\frac{\tau_{acc}}{\tau_m}\frac{\bar{h}_{acc}}{h_m}}\bar{h}_{acc} \quad (12)$$

are uniform and satisfy

$$\bar{v} = \frac{q_{in}}{\bar{\rho}} \quad (13)$$

as well as the fundamental diagram relation

$$\frac{1}{\bar{\rho}} - L = \bar{h}_{mix}\bar{v}. \quad (14)$$

To ensure this, first note that relations (1) and (3) imply that the equilibrium values for ρ and v, say ρ^e and v^e, respectively, satisfy $\rho^e(x)v^e(x) = q_{in}$, for all $x \in [0, D]$. From (2) and (4), it then follows, using (9), that the equilibrium profile of the speed satisfies the following ordinary differential equation (ODE) in x:

$$v^{e\prime}(x) = -\frac{1}{\tau_{mix}}\frac{v^e(x) + \frac{L}{\bar{h}_{mix} - \frac{1}{q_{in}}}}{v^e(x)} \quad (15)$$

with final condition $v^e(D) = -\frac{L}{\bar{h}_{mix} - \frac{1}{q_{in}}}$. Thus,

$$v^e(x) = \frac{L}{\frac{1}{q_{in}} - \bar{h}_{mix}} = \bar{v}, \quad \text{for all } x \in [0, D] \quad (16)$$

which can be seen noting that $v^{\mathrm{e}} = \bar{v}$ is an equilibrium of (15). In order to guarantee that $\rho_{\min} < \bar{\rho} < (1/L)$ $\forall \alpha \in [0, 1]$, which also implies from (13), (14) that $0 < \bar{v} < (1/\bar{h}_{\mathrm{mix}})((1/\rho_{\min}) - L) \leq v_{\mathrm{f}}$, we require that time gaps and inflow are such that relation $0 < q_{\mathrm{in}} < (v_{\mathrm{f}} h_{\min}/h_{\max}(L + v_{\mathrm{f}} h_{\min}))$ holds.

III. Control Design for the Linearized System

A. Linearization and Diagonalization of the System

We define the error variables $\tilde{\rho}(x,t) = \rho(x,t) - \bar{\rho}$, $\tilde{v}(x,t) = v(x,t) - \bar{v}$, and $\tilde{h}_{\mathrm{acc}}(x,t) = h_{\mathrm{acc}}(x,t) - \bar{h}_{\mathrm{acc}}$. Linearizing (1)–(4) around the uniform, congested equilibrium profile, we get

$$\tilde{\rho}_t(x,t) + \bar{v}\tilde{\rho}_x(x,t) + \bar{\rho}\tilde{v}_x(x,t) = 0 \tag{17}$$

$$\tilde{v}_t(x,t) - c_4\tilde{v}_x(x,t) = -c_1\tilde{\rho}(x,t) - c_2\tilde{v}(x,t) - c_3\tilde{h}_{\mathrm{acc}}(x,t) \tag{18}$$

$$\tilde{\rho}(0,t) + c_5\tilde{v}(0,t) = 0 \tag{19}$$

$$\tilde{v}_t(D,t) = -c_1\tilde{\rho}(D,t) - c_2\tilde{v}(D,t) - c_3\tilde{h}_{\mathrm{acc}}(D,t) \tag{20}$$

where $c_1 = (1/\bar{\rho}^2\tau_{\mathrm{mix}}\bar{h}_{\mathrm{mix}})$, $c_2 = (1/\tau_{\mathrm{mix}})$, $c_3 = (\alpha/\tau_{\mathrm{acc}}\bar{h}_{\mathrm{acc}}^2)((1/\bar{\rho}) - L)$, $c_4 = (L/\bar{h}_{\mathrm{mix}})$, and $c_5 = (\bar{\rho}/\bar{v})$. Defining $\tilde{z}(x) = e^{(c_2 x/\bar{v})}\big(\tilde{\rho}(x) + \bar{h}_{\mathrm{mix}}\bar{\rho}^2\tilde{v}(x)\big)$ and noting that $c_2 - c_1\bar{h}_{\mathrm{mix}}\bar{\rho}^2 = 0$, we rewrite systems (17)–(20) in a diagonal form as

$$\tilde{z}_t(x,t) + \bar{v}\tilde{z}_x(x,t) = -e^{\frac{c_2 x}{\bar{v}}}\bar{h}_{\mathrm{mix}}\bar{\rho}^2 c_3\tilde{h}_{\mathrm{acc}}(x,t) \tag{21}$$

$$\tilde{v}_t(x,t) - c_4\tilde{v}_x(x,t) = -c_1 e^{-\frac{c_2 x}{\bar{v}}}\tilde{z}(x,t) - c_3\tilde{h}_{\mathrm{acc}}(x,t) \tag{22}$$

$$\tilde{z}(0,t) = -L\frac{\bar{\rho}^2}{\bar{v}}\tilde{v}(0,t) \tag{23}$$

$$\tilde{v}_t(D,t) = -c_1 e^{-\frac{c_2}{\bar{v}}D}\tilde{z}(D,t) - c_3\tilde{h}_{\mathrm{acc}}(D,t). \tag{24}$$

B. Control Law

In addition to improving performance, feedback control is needed because systems (21)–(24) for $h_{\mathrm{acc}} = \bar{h}_{\mathrm{acc}}$ is unstable, as it is shown in the next proposition whose proof can be found in Appendix A.

Proposition 1: Systems (21)–(24) is exponentially unstable in open loop.

The control law is chosen as

$$h_{\mathrm{acc}}(x,t) = \bar{h}_{\mathrm{acc}} + \frac{1}{c_3}\Big(-c_1 e^{-\frac{c_2 x}{\bar{v}}}\tilde{z}(x,t) + k\tilde{v}(x,t)\Big) \tag{25}$$

$$= \bar{h}_{\mathrm{acc}} + \frac{1}{c_3}(-c_1\tilde{\rho}(x,t) + (k - c_2)\tilde{v}(x,t)) \tag{26}$$

with $k > 0$ being arbitrary, which gives

$$\tilde{z}_t(x,t) + \bar{v}\tilde{z}_x(x,t) = c_2\tilde{z}(x,t) - ke^{\frac{c_2 x}{\bar{v}}}\bar{h}_{\mathrm{mix}}\bar{\rho}^2\tilde{v}(x,t) \tag{27}$$

$$\tilde{v}_t(x,t) - c_4\tilde{v}_x(x,t) = -k\tilde{v}(x,t) \tag{28}$$

$$\tilde{z}(0,t) = -L\frac{\bar{\rho}^2}{\bar{v}}\tilde{v}(0,t) \tag{29}$$

$$\tilde{v}_t(D,t) = -k\tilde{v}(D,t). \tag{30}$$

From the closed-loop system (27)–(30), it is evident that the feedback law aims at eliminating the source term in (22), which may cause instability due to a feedback connection between the states $\tilde{z}$ and $\tilde{v}$ while rendering the $\tilde{v}(D)$ subsystem exponentially stable (and autonomous).

Taking into account that the traffic system operates in a congested regime, the operating point of the controller, as this is seen via the steady-state time gap for ACC-equipped vehicles $\bar{h}_{\mathrm{acc}}$, may vary considering, for example, safety, comfort, or TTT criteria. For instance, in cases in which safety is a primary goal, the time gap $\bar{h}_{\mathrm{acc}}$ may take large values [which implies that $\bar{h}_{\mathrm{mix}}$ also takes large values, according to (12)], whereas when comfort is of significant importance, no action (e.g., as recommendation to drivers of ACC-equipped vehicles or as direct manipulation of the ACC settings of individual vehicles) may be taken (in order to not disrupt the driver) from the controller for imposing the value of $\bar{h}_{\mathrm{acc}}$, which implies that the driver alone may set the value for the time-gap $\bar{h}_{\mathrm{acc}}$, see, e.g., [40]. Moreover, it may be beneficial, from a TTT point of view, for the time-gap $\bar{h}_{\mathrm{acc}}$ to take large values, since, for given inflow, lower steady-state densities may be achieved (via the achievement of higher steady-state speeds) as it can be seen from relations (13) and (16). We consider a specific scenario and further discuss about the choice of $\bar{h}_{\mathrm{acc}}$ (as well as of h_m) in Section V.

In practice, under a vehicle-to-infrastructure (V2I) communication paradigm, the control authority may implement the proposed strategy either as time-gap recommendations to drivers of ACC-equipped vehicles or via direct manipulation of the ACC settings of such vehicles, see, e.g., [40]. Furthermore, the developed feedback law, given in the simple formulae (26), requires measurements of the average speed and density (or, equivalently, average speed and flow, via the flow definition $q = \rho v$, in case flow measurements are available instead) throughout the spatial domain. This information could be obtained by the central control authority via utilization of connected vehicles[7] reports (e.g., reporting speed, position, or other information) as well as measurements from fixed detectors and, potentially, also employing certain traffic state estimation methodologies, see, e.g., [5], [11], [22], [47].

IV. Stability and Convective Stability Analyses

A. Stability in C^1 Norm

We establish the next stability in the stronger C^1 norm in order to guarantee additional stability properties for the closed-loop system that may be desirable from a traffic flow control viewpoint, see, e.g., [45]. Stability results in other norms, such as, for example, the L^2 norm, may be also obtained. The proofs of such results follow from the proof of the following theorem, which is provided in Appendix B.

Theorem 1: Consider a closed-loop system consisting of systems (17)–(20) and control law (26). For all initial conditions $(\tilde{\rho}(\cdot,0), \tilde{v}(\cdot,0)) \in C^1[0,D] \times C^1[0,D]$, which satisfy first-order compatibility with boundary conditions, there exists

[7] Besides ACC-equipped vehicles, a connected vehicle may be any vehicle able to exchange information with the central monitoring and control unit.

a positive constant μ such that the following holds[8] for all $t \geq 0$

$$\|\tilde{\rho}(t)\|_{C^1} + \|\tilde{v}(t)\|_{C^1} \leq \mu(\|\tilde{\rho}(0)\|_{C^1} + \|\tilde{v}(0)\|_{C^1})e^{-\frac{k}{2}t}. \tag{31}$$

B. Convective Stability in $\mathscr{L}_p$, $p \in [1, +\infty]$, Norm

Next, we study the convective stability properties of the closed-loop system, see, e.g., [6], [44], which is a notion related to string stability of a finite platoon of vehicles, see, e.g., [23], [42]. In a nutshell, convective stability in the present case guarantees that the magnitude (in $\mathscr{L}_p$ sense) of the deviation of speed as well as of its gradient, at some location (e.g., due to the presence of an unmodeled on-ramp at this specific location, acting as singular source), from the equilibrium point, decreases as the perturbation propagates backward in the spatial domain. Adopting an input-output approach, we establish the following result whose proof can be found in Appendix C.

Theorem 2: Systems (28) and (30) are $\mathscr{L}_p$, $p \in [1, \infty]$, convectively stable in the sense that for any $0 \leq x_2 < x_1 \leq D$ such that $\tilde{v}(x_1) \in \mathscr{L}_p$ and $\tilde{v}_x(x_1) \in \mathscr{L}_p$, the following holds:

$$\|\tilde{v}(x_2)\|_{\mathscr{L}_p} < \|\tilde{v}(x_1)\|_{\mathscr{L}_p} \tag{32}$$

$$\|\tilde{v}_x(x_2)\|_{\mathscr{L}_p} < \|\tilde{v}_x(x_1)\|_{\mathscr{L}_p}. \tag{33}$$

V. Simulation Results

A. Model Parameters and Numerical Implementation

The parameters of systems (1)–(4) utilized in the simulation investigations are shown in Table I.

The chosen parameters are considered reasonable for a traffic flow model, see, e.g., [6], [15], [21], [33]. In particular, we choose a value for the time gap of manually driven vehicles h_m that is close to the reported average values of about 1.2 s, see, e.g., [34], [40], but slightly lower than this to reflect evidence that drivers may follow a preceding vehicle at smaller time gaps in congested traffic, compared to the case of light traffic conditions, see, e.g., [34].

For the numerical solution of the hyperbolic systems (1)–(4) in open-loop as well as under (26), a modified Rusanov scheme, which is an explicit finite-volume scheme of centered type with added numerical diffusion, with time and spatial discretization steps of (1/30) s and (1/300) km, respectively, is employed, see, e.g., [19], [37]. The ODE (4) that corresponds to the downstream boundary condition for the speed is numerically solved utilizing a forward Euler method with the same time step. The upstream and downstream boundary values for density and speed, respectively, are obtained from the boundary conditions (3) and (4), whereas for obtaining the "missing" upstream and downstream boundary values for speed and density, respectively, we use fictitious cells, extrapolating the corresponding values from the interior of the domain.

[8]The assumptions of Theorem 1 imply that $(\tilde{z}(\cdot,0), \tilde{v}(\cdot,0)) \in C^1[0,D] \times C^1[0,D]$ satisfy the first-order compatibility, and thus, systems (27)–(30) exhibit a unique, classical solution such that $\tilde{z}, \tilde{v} \in C^1([0,D] \times [0,+\infty))$ (and hence, so does $\tilde{\rho}$), see, e.g., [3], [13], [38].

TABLE I
Parameters of Systems (1)–(4)

q_{in}	$1200\left(\frac{\text{veh}}{\text{h}}\right)$	τ_{acc}	2 (s)	h_{m}	1 (s)
$\rho_{\min}$	$37\left(\frac{\text{veh}}{\text{km}}\right)$	α	0.15	D	1000 (m)
τ_{m}	60 (s)	L	5 (m)		

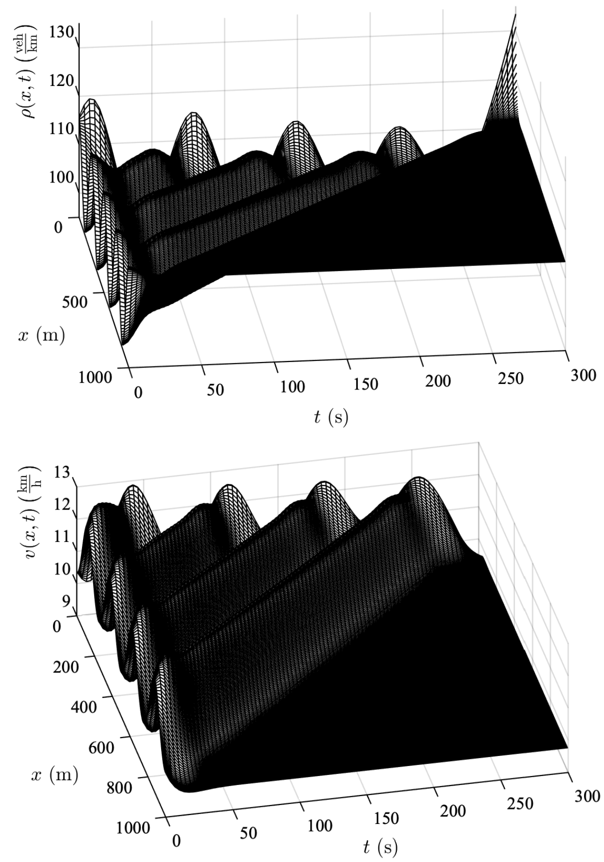

Fig. 3. Open-loop response of systems (1)–(4) with parameters as in Table I for $\bar{h}_{\text{acc}} = 1.5$ and initial conditions $\rho(x,0) = \bar{\rho} + 10\cos(8\pi x/D)$, $v(x,0) = (q_{\text{in}}/\rho(x,0))$.

B. Controller's Parameters and Performance Evaluation

The operating point of the traffic system, as it is dictated by the steady-state value of the mixed time gap according to (12), it is selected such that $\bar{h}_{\text{acc}} = 1.5$ s. Such a value reflects the fact that the equilibrium of the time gap for ACC-equipped vehicles may be dictated from drivers' choices rather than from interventions of the control authority, for a control strategy that aims at minimizing controller's interventions, which may be disrupting for the driver. Consequently, we choose a value for $\bar{h}_{\text{acc}}$ that is close to what drivers of ACC-equipped vehicles set in congested conditions, which is evidenced to be larger compared to manual driving in heavy traffic and which is reported to be around the selected value, see, e.g., [34].

The steady-state values for density and speed are derived from (13), (14) as $\bar{\rho} = 105.8$ (veh/km), $\bar{v} = 11.35$ (km/h). Fig. 3 shows the open-loop response for initial conditions $\rho(x,0) = \bar{\rho} + 10\cos((8\pi x/D))$, $v(x,0) = (q_{\text{in}}/\rho(x,0))$. From Fig. 3, it is evident that the open-loop response exhibits

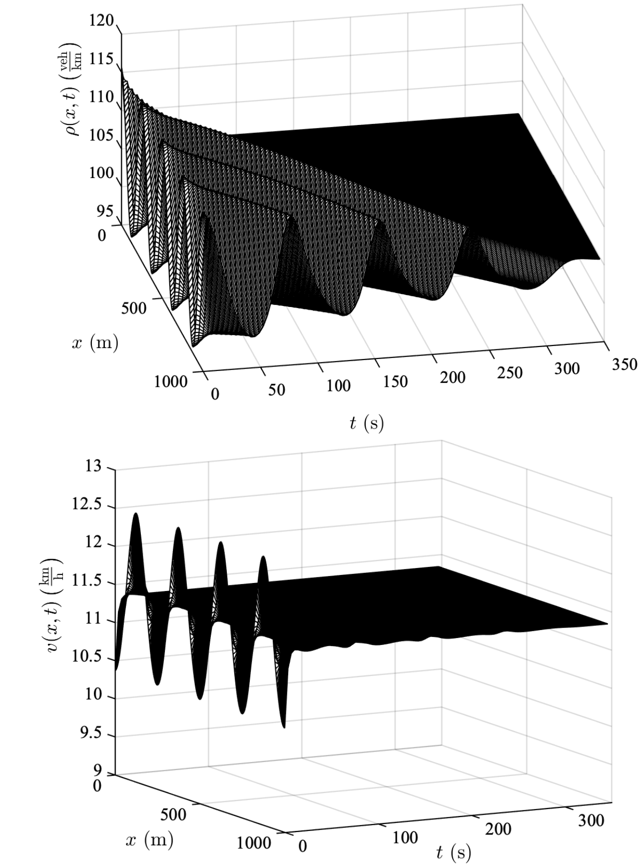

Fig. 4. Closed-loop response of systems (1)–(4) with parameters shown in Table I, under the feedback law (26) with $k = 0.25$, for $\bar{h}_{\text{acc}} = 1.5$ and initial conditions $\rho(x,0) = \bar{\rho} + 10\cos(8\pi x/D)$, $v(x,0) = (q_{\text{in}}/\rho(x,0))$.

an unstable and quite oscillatory behavior. In fact, the initial deviation from the uniform, equilibrium profile, which has a sinusoidal shape to imitating stop-and-go initial traffic conditions, propagates backward without being attenuated, eventually leading to an increase in density and a corresponding decrease in speed. On the contrary, as it is shown in Fig. 4, the traffic flow is stabilized and, in particular, the oscillations (stop-and-go waves) in the speed response are considerably suppressed when the feedback law (26) is applied. The control effort (26) for $k = 0.25$ (1/s) is shown in Fig. 5, from which one can also observe that the resulting values for the time gap of ACC-equipped vehicles lie within the bounds typically implemented in ACC-equipped vehicles settings, namely, approximately within the interval [0.8, 2.2] s, see, e.g., [34], [40].

To quantify the benefits of controller (26), we compare the performances of the closed- and open-loop systems in terms of fuel consumption, comfort, and TTT. We use the following performance indices, see, e.g., [44, Ch. 21]:

$$J_{\text{fuel}} = \int_0^T \int_0^D \bar{J}_{\text{fuel}}(v(x,t), a(x,t))\rho(x,t)dxdt \quad (34)$$

$$J_{\text{comfort}} = \int_0^T \int_0^D \left(a(x,t)^2 + a_t(x,t)^2\right)\rho(x,t)dxdt \quad (35)$$

$$J_{\text{TTT}} = \int_0^T \int_0^D \rho(x,t)dxdt \quad (36)$$

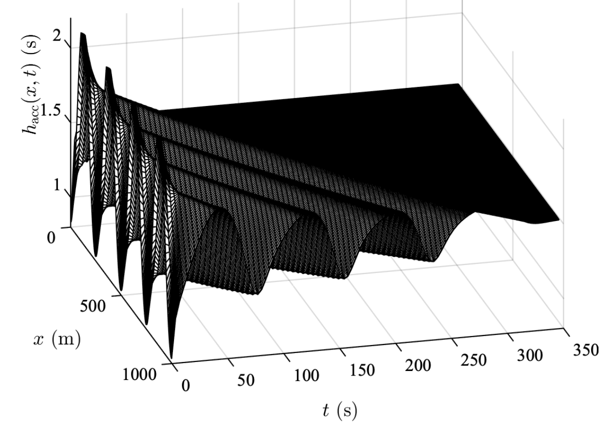

Fig. 5. Feedback control law (26) with $k = 0.25$ and $\bar{h}_{\text{acc}} = 1.5$.

TABLE II
PERFORMANCE INDICES (34)–(36)

Performance index	Percentage (%) improvement with (26)
J_{fuel}	4.2
J_{comfort}	95
J_{TTT}	4.3

where $\bar{J}_{\text{fuel}}(v,a) = \max\{0, b_0 + b_1 v + b_3 v^3 + b_4 v a\}$, $a = v_t + v v_x$, $T = 350$ s, and b_0, b_1, b_3, b_4 are provided in [44, p. 485]. Application of the controller results in better performance in all of the metrics, as it is shown in Table II. In particular, the improvement in fuel consumption and comfort is attributed to the fast homogenization of the speed field. The improvement in fuel consumption and TTT may be best appreciated taking also into account the cost of congestion, see, e.g., [20], and the considered setup's scale.

VI. CONCLUSION AND FUTURE WORK

We presented a control design methodology for stabilization of traffic flow in a congested regime exploiting the capabilities of vehicles with ACC features and utilizing an ARZ-type model for mixed traffic. The closed-loop system, under the developed control law, was shown to be exponentially stable as well as convectively stable. The numerical investigation showed that the performance of the considered traffic system, under the proposed controller, is improved and the improvement, in terms of fuel consumption, travel time, and comfort, was quantified utilizing various performance indices.

The control design approach presented is based on a linear version of the original nonlinear system. As a next step, it would be interesting to consider the nonlinear, feedback control design problem as well as to perform the analysis in a nonlinear setting considering the nonlinear closed-loop system (potentially obtaining an explicit estimate of the region of attraction of the controller and studying its input-to-state stability properties), similar to, e.g., [3], [12], [14], [26]. It would be also interesting to consider problems on circular spatial domains, as it is the case, for example, in [41], employing a microscopic framework. Furthermore, one could, in principle, utilize the Lyapunov tools presented to study the robustness of the control law to small parametric uncertainties, as well as pursue an output-feedback control design under various measurement configurations. Last but not least, the accuracy of the presented control-oriented model may be validated with traffic data generated from a microscopic simulation platform (see, e.g., [40]).

Appendix A
Proof of Proposition 1

We start computing the characteristic equation of systems (21)–(24) when $\tilde{h}_{\mathrm{acc}} \equiv 0$. One may proceed either utilizing the Laplace transform and capitalizing on the relation of systems (21)–(24) to a delay system, see, e.g., [2], or computing the eigenvalues of the generator associated with systems (21)–(24), see, e.g., [3], [32]. We proceed using the latter approach. Defining $\tilde{z}(x,t) = e^{\sigma t}\phi(x)$ and $\tilde{v}(x,t) = e^{\sigma t}\psi(x)$, $\sigma \in \mathbb{C}$, one can conclude from (21)–(24) that the following boundary-value problem should be satisfied:

$$\phi'(x) = -\frac{\sigma}{\bar{v}}\phi(x); \quad \psi'(x) = \frac{\sigma}{c_4}\psi(x) + \frac{c_1}{c_4}e^{-\frac{c_2 x}{\bar{v}}}\phi(x) \quad \text{(A.1)}$$

$$\phi(0) = -L\frac{\bar{\rho}^2}{\bar{v}}\psi(0); \quad \phi(D) = -\frac{\sigma}{c_1}e^{\frac{c_2 D}{\bar{v}}}\psi(D). \quad \text{(A.2)}$$

Solving (A.1) and using the boundary conditions (A.2), one can conclude that, in order for nontrivial solutions to (A.1), (A.2) to exist, σ should satisfy the following relation:

$$-a_1 e^{-\sigma\tau D} + \sigma\tau_{\mathrm{mix}}c_1 - \sigma c_1 \frac{1 - e^{-\sigma\tau D}e^{-\frac{c_2 D}{\bar{v}}}}{\sigma\tau\bar{v} + c_2} = 0 \quad \text{(A.3)}$$

where $a_1 = (1/\bar{v})c_4 c_1 e^{-(c_2 D/\bar{v})}$ and $\tau = (1/c_4) + (1/\bar{v})$. We next prove that (A.3) always admits a real solution within an interval (σ_1, σ_2) for some $\sigma_1, \sigma_2 > 0$. Since $c_2 > 0$, for $\sigma \in [0, +\infty)$ relation (A.3) is equivalent to $a_2\sigma^2 - a_1(\sigma + c_2)e^{-\sigma\tau D} = 0$, where $a_2 = \bar{v}c_1\tau_{\mathrm{mix}}\tau$. The proof is completed observing that $f(\sigma) = a_2\sigma^2 - a_1(\sigma + c_2)e^{-\sigma\tau D}$ is continuous for all $\sigma \geq 0$ as well as that $f(0) = -a_1 c_2 < 0$ and $\lim_{\sigma+\infty} f(\sigma) = +\infty$.

Appendix B
Proof of Theorem 1

We start defining the following functionals:

$$V_{1_p}(t) = \int_0^D e^{-2k_1 p x}\tilde{z}(x,t)^{2p}dx + \int_0^D e^{-2k_1 p x}\tilde{z}_x(x,t)^{2p}dx \quad \text{(B.1)}$$

$$V_{2_p}(t) = \int_0^D e^{2k_2 p x}\tilde{v}(x,t)^{2p}dx + \int_0^D e^{2k_2 p x}\tilde{v}_x(x,t)^{2p}dx \quad \text{(B.2)}$$

$$V_{3_p}(t) = \tilde{v}(D,t)^{2p} \quad \text{(B.3)}$$

where k_1, k_2 are arbitrary positive constants and p is a positive integer. Moreover, from systems (27)–(30), we obtain

$$\tilde{z}_{xt}(x,t) + \bar{v}\tilde{z}_{xx}(x,t) = c_2\tilde{z}_x(x,t) - ke^{\frac{c_2 x}{\bar{v}}}\bar{h}_{\mathrm{mix}}\bar{\rho}^2\tilde{v}_x(x,t) - \frac{c_2}{\bar{v}}ke^{\frac{c_2 x}{\bar{v}}}\bar{h}_{\mathrm{mix}}\bar{\rho}^2\tilde{v}(x,t) \quad \text{(B.4)}$$

$$\tilde{v}_{xt}(x,t) - c_4\tilde{v}_{xx}(x,t) = -k\tilde{v}_x(x,t) \quad \text{(B.5)}$$

$$\tilde{z}_x(0,t) = L\frac{\bar{\rho}^2}{\bar{v}^2}c_4\tilde{v}_x(0,t) - \frac{k\bar{\rho}^2}{\bar{v}} \times \left(\bar{h}_{\mathrm{mix}} + \frac{L}{\bar{v}} + L\frac{c_2}{\bar{v}k}\right)\tilde{v}(0,t) \quad \text{(B.6)}$$

$$\tilde{v}_x(D,t) = 0. \quad \text{(B.7)}$$

Differentiating (B.1)–(B.3) along (27)–(30), (B.4)–(B.7), with integration by parts, Young's inequality and as $(d_1 + d_2)^p \leq 2^p\left(d_1^p + d_2^p\right)\ \forall\, d_1, d_2, p > 0$, with p integer, we get

$$\begin{aligned}\dot{V}_{1_p}(t) \leq{}& -\bar{v}e^{-2k_1 pD}\tilde{z}(D,t)^{2p} + \left(c_7^{2p} + c_9^{2p}\right)\bar{v}\tilde{v}(0,t)^{2p} \\ &-2p\left(\bar{v}k_1 - c_2 - \frac{2p-1}{2p}c_6\right)V_{1_p}(t) + c_6 V_{2_p}(t) \\ &- \bar{v}e^{-2k_1 pD}\tilde{z}_x(D,t)^{2p} + c_8^{2p}\bar{v}\tilde{v}_x(0,t)^{2p}\end{aligned} \quad \text{(B.8)}$$

$$\begin{aligned}\dot{V}_{2_p}(t) ={}& c_4 e^{2k_2 pD}V_{3_p}(t) - c_4\tilde{v}(0,t)^{2p} - c_4\tilde{v}_x(0,t)^{2p} \\ &- 2p(k + c_4 k_2)V_{2_p}(t)\end{aligned} \quad \text{(B.9)}$$

$$\dot{V}_{3_p}(t) = -2pkV_{3_p}(t) \quad \text{(B.10)}$$

with $c_6 = ke^{(c_2 D/\bar{v})}\bar{h}_{\mathrm{mix}}\bar{\rho}^2(1 + (c_2/\bar{v}))$, $c_7 = L(\bar{\rho}^2/\bar{v})$, $c_8 = 2L(\bar{\rho}^2/\bar{v}^2)c_4$, $c_9 = 2(k\bar{\rho}^2/\bar{v})\left(\bar{h}_{\mathrm{mix}} + (L/\bar{v}) + L(c_2/\bar{v}k)\right)$. Defining the Lyapunov functional

$$V_p(t) = V_{1_p}(t) + k_3{}^{2p}V_{2_p}(t) + k_4{}^{2p}e^{2k_2 pD}V_{3_p}(t), \quad \text{(B.11)}$$

we obtain from (B.8)–(B.10)

$$\begin{aligned}\dot{V}_p(t) \leq{}& -\left(k_3{}^{2p}c_4 - c_7^{2p}\bar{v} - c_9^{2p}\bar{v}\right)\tilde{v}(0,t)^{2p} \\ &- 2p\left(\bar{v}k_1 - c_2 - \frac{2p-1}{2p}c_6\right)V_{1_p}(t) \\ &- \left(2pk_3^{2p}(k + c_4 k_2) - c_6\right)V_{2_p}(t) \\ &- \left(2pkk_4{}^{2p} - k_3{}^{2p}c_4\right)e^{2k_2 pD}V_{3_p}(t) \\ &- \left(k_3{}^{2p}c_4 - c_8^{2p}\bar{v}\right)\tilde{v}_x(0,t)^{2p}.\end{aligned} \quad \text{(B.12)}$$

Since $p \geq 1$, choosing $k_1 = (1/\bar{v})(c_2 + c_6 + k)$, $k_2 = (c_6/2c_4)$, $k_3 = \max\{(c_7 + c_8 + c_9)\max\{(\bar{v}/c_4), 1\}, 1\}$, and $k_4 = k_3\max\{(c_4/k), 1\}$, we get from (B.12) that $\dot{V}_p(t) \leq -2pkV_{1_p}(t) - 2pkk_3{}^{2p}V_{2_p}(t) - pkk_4{}^{2p}e^{2k_2 pD}V_{3_p}(t)$. Hence, using (B.11) we arrive at[9]

$$\dot{V}_p(t) \leq -pkV_p(t). \quad \text{(B.13)}$$

From (B.13), we then get $V_p^{(1/2p)}(t) \leq e^{-(k/2)t}V_p^{(1/2p)}(0)$, and thus, using (B.11) we obtain $V_{1_p}^{(1/2p)}(t) + k_3 V_{2_p}^{(1/2p)}(t) + k_4 e^{k_2 D}V_{3_p}^{(1/2p)}(t) \leq 4e^{-(k/2)t}(V_{1_p}^{(1/2p)}(0) + k_3 V_{2_p}^{(1/2p)}(0) + k_4 e^{k_2 D}V_{3_p}^{(1/2p)}(0))$. With definitions (B.1)–(B.3) and standard inequalities, we get

$$\Xi_p(t) \leq 8e^{-\frac{k}{2}t}\,\Xi_p(0) \quad \text{(B.14)}$$

$$\begin{aligned}\Xi_p(t) ={}& \|\tilde{z}(t)\|_{-k_1,2p} + k_3\|\tilde{v}(t)\|_{k_2,2p} + \|\tilde{z}_x(t)\|_{-k_1,2p} \\ &+ k_3\|\tilde{v}_x(t)\|_{k_2,2p} + k_4 e^{k_2 D}|\tilde{v}(D,t)|.\end{aligned} \quad \text{(B.15)}$$

Taking the limit of (B.14) as $p \to +\infty$, with the definition of the supremum norm and (B.15), we get $\|\tilde{z}(t)\|_{C^1} + \|\tilde{v}(t)\|_{C^1} +$

[9] To derive (B.13) we also used (B.4), (B.5), which implies that, in principle, higher regularity of solutions is needed. Yet, one could show that (B.13) still holds (in the sense of distributions), using similar arguments to, e.g., [3].

$|\tilde{v}(D,t)| \leq \bar{\mu}(\|\tilde{z}(0)\|_{C^1} + \|\tilde{v}(0)\|_{C^1} + |\tilde{v}(D,0)|)e^{-(k/2)t}$, for some positive constant $\bar{\mu}$, where we also used the facts that $e^{-k_1 D}\|\tilde{z}(t)\|_C \leq \|\tilde{z}(t)\|_{-k_1,C} \leq \|\tilde{z}(t)\|_C$ and $\|\tilde{v}(t)\|_C \leq \|\tilde{v}(t)\|_{k_2,C} \leq e^{k_2 D}\|\tilde{v}(t)\|_C$. The proof is completed using the relation $\tilde{z}(x) = e^{(c_2 x/\bar{v})}\big(\tilde{\rho}(x) + \bar{h}_{\text{mix}}\bar{\rho}^2\tilde{v}(x)\big)$.

Appendix C
Proof of Theorem 2

Taking the Laplace transform of (28) and setting the initial condition to zero, we obtain

$$\tilde{V}(x,s) = e^{-\frac{k}{c_4}(x_1 - x)}e^{-\frac{s}{c_4}(x_1 - x)}\tilde{V}(x_1,s) \tag{C.1}$$

for all $0 \leq x \leq x_1 \leq D$, and thus,

$$\tilde{v}(x_2,t) = e^{-\frac{k}{c_4}(x_1 - x_2)}\tilde{v}\left(x_1, t + \frac{x_2 - x_1}{c_4}\right) \tag{C.2}$$

where $\tilde{v}(x_1,\theta)$, within the interval $((x_2 - x_1)/c_4) \leq \theta < 0$, is set to zero, as, in the present context, we are concerned with an input-output representation (without accounting for the effect of initial conditions), in which $\tilde{v}(x_1,t)$ is viewed as input signal (with initial condition $\tilde{v}(x_1,\theta)$, $((x_2 - x_1)/c_4) \leq \theta < 0$). Therefore, from (C.2), we get that $(\int_0^{+\infty}|\tilde{v}(x_2,t)|^p dt)^{(1/p)} = e^{-(k/c_4)(x_1-x_2)}(\int_0^{+\infty}|\tilde{v}(x_1, t + ((x_2 - x_1)/c_4))|^p dt)^{(1/p)}$. Since $k, c_4 > 0$ and $x_2 < x_1$, we obtain (32) for $p \in [1,+\infty)$. Similarly, taking a supremum over time in (C.2), we obtain (32) for $p = +\infty$. Differentiating (C.1) with respect to x, we get $\tilde{V}'(x,s) = e^{-(k/c_4)(x_1-x)}e^{-(s/c_4)(x_1-x)}\tilde{V}'(x_1,s)$, for all $0 \leq x \leq x_1 \leq D$. Thus, employing identical arguments, we obtain (33).

Acknowledgment

The authors would like to thank Dr. Diamantis Manolis, Prof. Markos Papageorgiou, and Prof. Claudio Roncoli for fruitful discussions.

References

[1] K. Ahn, A. A. Trani, H. Rakha, and M. Van Aerde, "Microscopic fuel consumption and emission models," in *Proc. Annu. Meeting Transp. Res. Board*. Washington, DC, USA: CD-ROM, 1999.

[2] J. Auriol, F. Bribiesca-Argomedo, D. Bou Saba, M. Di Loreto, and F. Di Meglio, "Delay-robust stabilization of a hyperbolic PDE-ODE system," *Automatica*, vol. 95, pp. 494–502, 2018.

[3] G. Bastin and J.-M. Coron, *Stability and Boundary Stabilization of 1-D Hyperbolic Systems*. Basel, Switzerland: Birkhäuser, 2016.

[4] N. Bekiaris-Liberis and A. M. Bayen, "Nonlinear local stabilization of a viscous Hamilton–Jacobi PDE," *IEEE Trans. Autom. Control*, vol. 60, no. 6, pp. 1698–1703, Jun. 2014.

[5] N. Bekiaris-Liberis, C. Roncoli, and M. Papageorgiou, "Highway traffic state estimation per lane in the presence of connected vehicles," *Transp. Res. B, Methodol.*, vol. 106, pp. 1–28, Dec. 2017.

[6] F. Belletti, M. Huo, X. Litrico, and A. M. Bayen, "Prediction of traffic convective instability with spectral analysis of the Aw–Rascle–Zhang model," *Phys. Lett. A*, vol. 379, no. 38, pp. 2319–2330, Oct. 2015.

[7] S. Blandin, X. Litrico, M. L. Delle Monache, B. Piccoli, and A. Bayen, "Regularity and Lyapunov stabilization of weak entropy solutions to scalar conservation laws," *IEEE Trans. Autom. Control*, vol. 62, no. 4, pp. 1620–1635, Apr. 2017.

[8] A. Bose and P. Ioannou, "Mixed manual/semi-automated traffic: A macroscopic analysis," *Transp. Res. C, Emerg. Technol.*, vol. 11, no. 6, pp. 439–462, Dec. 2003.

[9] C. Chen, Z. Jia, and P. Varaiya, "Causes and cures of highway congestion," *IEEE Control Syst.*, vol. 21, no. 6, pp. 26–32, Dec. 2001.

[10] C. Claudel and A. Bayen, "Lax-Hopf based incorporation of internal boundary conditions into Hamilton–Jacobi equation—Part I: Theory," *IEEE Trans. Autom. Control*, vol. 55, no. 5, pp. 1142–1157, May 2010.

[11] C. G. Claudel and A. M. Bayen, "Lax–Hopf based incorporation of internal boundary conditions into Hamilton–Jacobi equation. Part II: Computational methods," *IEEE Trans. Autom. Control*, vol. 55, no. 5, pp. 1158–1174, May 2010.

[12] R. Vazquez, J.-M. Coron, M. Krstic, and G. Bastin, "Local exponential H^2 stabilization of a 2×2 quasilinear hyperbolic system using backstepping," in *Proc. IEEE Conf. Decis. Control Eur. Control Conf.*, Dec. 2011, pp. 1329–1334.

[13] R. Courant and D. Hilbert, *Methods of Mathematical Physics: Partial Differential Equations*. New York, NY, USA: Interscience, 1962.

[14] J. de Halleux, C. Prieur, J.-M. Coron, B. d'Andréa-Novel, and G. Bastin, "Boundary feedback control in networks of open channels," *Automatica*, vol. 39, no. 8, pp. 1365–1376, Aug. 2003.

[15] A. I. Delis, I. K. Nikolos, and M. Papageorgiou, "Macroscopic traffic flow modeling with adaptive cruise control: Development and numerical solution," *Comput. Math. Appl.*, vol. 70, no. 8, pp. 1921–1947, Oct. 2015.

[16] M. L. Delle Monache, B. Piccoli, and F. Rossi, "Traffic regulation via controlled speed limit," *SIAM J. Control Optim.*, vol. 55, no. 5, pp. 2936–2958, Jan. 2017.

[17] C. Diakaki, M. Papageorgiou, I. Papamichail, and I. Nikolos, "Overview and analysis of vehicle automation and communication systems from a motorway traffic management perspective," *Transp. Res. A, Policy Pract.*, vol. 75, pp. 147–165, May 2015.

[18] F. Di Meglio, F. B. Argomedo, L. Hu, and M. Krstic, "Stabilization of coupled linear heterodirectional hyperbolic PDE–ODE systems," *Automatica*, vol. 87, pp. 281–289, Jan. 2018.

[19] V. Dolejší and T. Gallouët, "A numerical study of a particular non-conservative hyperbolic problem," *Comput. Fluids*, vol. 37, no. 9, pp. 1077–1091, Oct. 2008.

[20] M. Errampalli, V. Senathipathi, and D. Thamban, "Effect of congestion on fuel cost and travel time cost on multi-lane highways in India," *Int. J. Traffic Transp. Eng.*, vol. 5, no. 4, pp. 458–472, Dec. 2015.

[21] S. Fan *et al.*, "Comparative model accuracy of a data-fitted generalized Aw-Rascle-Zhang model," *Netw. Heterogeneous Media*, vol. 9, no. 2, pp. 239–268, 2014.

[22] M. Fountoulakis, N. Bekiaris-Liberis, C. Roncoli, I. Papamichail, and M. Papageorgiou, "Highway traffic state estimation with mixed connected and conventional vehicles: Microscopic simulation-based testing," *Transp. Res. C, Emerg. Technol.*, vol. 78, pp. 13–33, May 2017.

[23] J. I. Ge and G. Orosz, "Dynamics of connected vehicle systems with delayed acceleration feedback," *Transp. Res. C, Emerg. Technol.*, vol. 46, pp. 46–64, Sep. 2014.

[24] P. Goatin, S. Göttlich, and O. Kolb, "Speed limit and ramp meter control for traffic flow networks," *Eng. Optim.*, vol. 48, no. 7, pp. 1121–1144, Jul. 2016.

[25] M. Herty and W.-A. Yong, "Feedback boundary control of linear hyperbolic systems with relaxation," *Automatica*, vol. 69, pp. 12–17, Jul. 2016.

[26] I. Karafyllis, N. Bekiaris-Liberis, and M. Papageorgiou, "Feedback control of nonlinear hyperbolic PDE systems inspired by traffic flow models," *IEEE Trans. Autom. Control*, vol. 64, no. 9, pp. 3647–3662, Sep. 2019.

[27] A. Kesting, M. Treiber, M. Schönhof, and D. Helbing, "Adaptive cruise control design for active congestion avoidance," *Transp. Res. C, Emerg. Technol.*, vol. 16, no. 6, pp. 668–683, Dec. 2008.

[28] O. Kolb, S. Göttlich, and P. Goatin, "Capacity drop and traffic control for a second order traffic model," *Netw. Heterogeneous Media*, vol. 12, pp. 663–681, Oct. 2017.

[29] P.-O. Lamare and N. Bekiaris-Liberis, "Control of 2×2 linear hyperbolic systems: Backstepping-based trajectory generation and PI-based tracking," *Syst. Control Lett.*, vol. 86, pp. 24–33, Dec. 2015.

[30] P. Y. Li, R. Horowitz, L. Alvarez, J. Frankel, and A. M. Robertson, "An automated highway system link layer controller for traffic flow stabilization," *Transp. Res. C, Emerg. Technol.*, vol. 5, no. 1, pp. 11–37, Feb. 1997.

[31] X. Litrico and V. Fromion, "Boundary control of hyperbolic conservation laws using a frequency domain approach," *Automatica*, vol. 45, pp. 647–656, Mar. 2009.

[32] A. F. Neves, H. de Souza Ribeiro, and O. Lopes, "On the spectrum of evolution operators generated by hyperbolic systems," *J. Funct. Anal.*, vol. 67, no. 3, pp. 320–344, Jul. 1986.

[33] D. Ngoduy, "Instability of cooperative adaptive cruise control traffic flow: A macroscopic approach," *Commun. Nonlinear Sci. Numer. Simul.*, vol. 18, no. 10, pp. 2838–2851, Oct. 2013.

[34] C. Nowakowski *et al.*, *Cooperative Adaptive Cruise Control: Testing Drivers' Choices of Following Distances*. Richmond, CA, USA: California PATH, 2011.

[35] G. Piacentini, P. Goatin, and A. Ferrara, "Traffic control via moving bottleneck of coordinated vehicles," *IFAC-PapersOnLine*, vol. 51, no. 9, pp. 13–18, 2018.

[36] C. Prieur and J. J. Winkin, "Boundary feedback control of linear hyperbolic systems: Application to the Saint-Venant–Exner equations," *Automatica*, vol. 89, pp. 44–51, Mar. 2018.

[37] V. V. Rusanov, "Calculation of interaction of non-steady shock waves with obstacles," *J. Comput. Math. Phys. USSR*, vol. 1, no. 2, pp. 267–279, 1961.

[38] D. L. Russell, "Quadratic performance criteria in boundary control of linear symmetric hyperbolic systems," *SIAM J. Control*, vol. 11, no. 3, pp. 475–509, Aug. 1973.

[39] W. J. Schakel and B. van Arem, "Improving traffic flow efficiency by in-car advice on lane, speed, and headway," *IEEE Trans. Intell. Transp. Syst.*, vol. 15, no. 4, pp. 1597–1606, Aug. 2014.

[40] A. Spiliopoulou, D. Manolis, F. Vandorou, and M. Papageorgiou, "Adaptive cruise control operation for improved motorway traffic flow," *Transp. Res. Rec.*, vol. 2672, no. 22, pp. 24–35, Dec. 2018.

[41] R. E. Stern *et al.*, "Dissipation of stop-and-go waves via control of autonomous vehicles: Field experiments," *Transp. Res. C, Emerg. Technol.*, vol. 89, pp. 205–221, Apr. 2018.

[42] D. Swaroop and J. K. Hedrick, "String stability of interconnected systems," *IEEE Trans. Autom. Control*, vol. 41, no. 3, pp. 349–357, Mar. 1996.

[43] S. Darbha and K. R. Rajagopal, "Intelligent cruise control systems and traffic flow stability," *Transp. Res. C, Emerg. Technol.*, vol. 7, no. 6, pp. 329–352, Dec. 1999.

[44] M. Treiber and A. Kesting, *Traffic Flow Dynamics–Data, Models and Simulation*. Berlin, Germany: Springer, 2013.

[45] J. Yi and R. Horowitz, "Macroscopic traffic flow propagation stability for adaptive cruise controlled vehicles," *Transp. Res. C, Emerg. Technol.*, vol. 14, no. 2, pp. 81–95, Apr. 2006.

[46] R. Vazquez and M. Krstic, "Marcum -functions and explicit kernels for stabilization of linear hyperbolic systems with constant coefficients," *Syst. Control Lett.*, vol. 68, pp. 33–42, Jun. 2014.

[47] R. Wang, Y. Li, and D. B. Work, "Comparing traffic state estimators for mixed human and automated traffic flows," *Transp. Res. C, Emerg. Technol.*, vol. 78, pp. 95–110, May 2017.

[48] H. Yu, S. Koga, and M. Krstic, "Stabilization of traffic flow with a leading autonomous vehicle," in *Proc. ASME DSCC*, Atlanta, GA, USA, 2018, p. 10.

[49] H. Yu and M. Krstic, "Traffic congestion control for Aw–Rascle–Zhang model," *Automatica*, vol. 100, pp. 38–51, Feb. 2019.

[50] H. Yu and M. Krstic, "Traffic congestion control on two-lane Aw–Rascle–Zhang model," in *Proc. IEEE CDC*, Miami Beach, FL, USA, Dec. 2018, pp. 2144–2149.

[51] H. M. Zhang, "A non-equilibrium traffic model devoid of gas-like behavior," *Transp. Res. B, Methodol.*, vol. 36, no. 3, pp. 275–290, Mar. 2002.

[52] L. Zhang and C. Prieur, "Necessary and sufficient conditions on the exponential stability of positive hyperbolic systems," *IEEE Trans. Autom. Control*, vol. 62, no. 7, pp. 3610–3617, Jul. 2017.

[53] L. Zhang and C. Prieur, "Stochastic stability of Markov jump hyperbolic systems with application to traffic flow control," *Automatica*, vol. 86, pp. 29–37, Dec. 2017.